Journal of Power Sources 185 (2008) 627–632

Contents lists available at ScienceDirect

Journal of Power Sources

journal homepage: www.elsevier.com/locate/jpowsour

Ni–Pt/C as anode electrocatalyst for a direct borohydride fuel cell

Xiaoying Geng[a,b], Huamin Zhang[a,*], Wei Ye[a,b], Yuanwei Ma[a,b], Hexiang Zhong[a]

[a] Lab of PEMFC Key Materials and Technologies, Dalian Institute of Chemical Physics, Chinese Academy of Sciences, Dalian 116023, China
[b] Graduate School of the Chinese Academy of Sciences, Beijing 100039, China

ARTICLE INFO

Article history:
Received 3 September 2008
Accepted 4 September 2008
Available online 16 September 2008

Keywords:
Direct borohydride fuel cell
Ni–Pt catalyst
Anode
Borohydride oxidation

ABSTRACT

In this study, a series of Ni–Pt/C and Ni/C catalysts, which were employed as anode catalysts for a direct borohydride fuel cell (DBFC), were prepared and investigated by XRD, TEM, cyclic voltammetry, chronopotentiometry and fuel cell test. The particle size of Ni_{37}–Pt_3/C (mass ratio, Ni:Pt = 37:3) catalyst was sharply reduced by the addition of ultra low amount of Pt. And the electrochemical measurements showed that the electro-catalytic activity and stability of the Ni_{37}–Pt_3/C catalysts were improved compared with Ni/C catalyst. The DBFC employing Ni_{37}–Pt_3/C catalyst on the anode (metal loading, 1 mg cm^{-2}) showed a maximum power density of 221.0 mW cm^{-2} at 60 °C, while under identical condition the maximum power density was 150.6 mW cm^{-2} for Ni/C. Furthermore, the polarization curves and hydrogen evolution behaviors on all the catalysts were investigated on the working conditions of the DBFC.

1. Introduction

Direct borohydride fuel cell (DBFC) is currently under increasing interests as a potential candidate for portable application due to high energy density of borohydride and easy handling of liquid fuel. The anode reaction of the DBFC is the direct oxidation of borohydride in alkaline medium:

$$BH_4^- + 8OH^- \rightarrow BO_2^- + 6H_2O + 8e^-, \quad E^0 = -1.24\,V \qquad (1)$$

When oxygen is employed as the oxidant in the cathode, the overall fuel cell reaction is:

$$BH_4^- + 2O_2 \rightarrow BO_2^- + 2H_2O, \quad E^0_{cell} = 1.64\,V \qquad (2)$$

The theoretical cell voltage is 1.64 V, higher than with a hydrogen or methanol anode. At 100% fuel efficiency, the specific capacity and energy density of $NaBH_4$ can reach 5.67 Ah g^{-1} and 9296 Wh kg^{-1}, respectively. The potential high energy density and power output of DBFC attract rapidly growing researches.

Electrocatalyst is one of the key materials of DBFC. Many catalysts such as noble metals (Pt, Pd, Au, Ag, Os) [1–15], transition metals (Ni, Cu) [1,6,16–20,24] and hydrogen storage alloys [18,21–23] have been evaluated as anode catalysts for DBFC. The direct oxidation of borohydride involves eight electrons (8e) per molecule in principle (Eq. (1)), while in practice the 8e oxidation is only observed on Au electrode [7,9,11,12]. However, the Au electrode usually demonstrates slow electrode kinetics and thus low current and power output [6,8,11,12]. From the view of fuel cell power output, anode materials such as Ni, Pt and Pd demonstrate fast electrode kinetics and thus good power performances. Considering the high cost of the noble metals such as Pt and Pd, Ni-based catalysts may be worthwhile to be further studied as anode catalysts, although the coulombic efficiencies are low due to hydrogen evolution [1,17,18–20]. But Li et al. [17] have found that the hydrogen evolution on Ni catalyst could be depressed by anode modification.

Most of the Ni electrodes used in the literatures were commercial Raney Ni or Ni powder [1,6,16–20]. Although supported catalysts are cost-effective and often have higher catalytic activities than unsupported catalysts [4], supported Ni catalysts are rarely studied in DBFC. Carbon supported Ni catalyst was only evaluated as anode catalyst in DBFC by Cheng et al. [25], and it was found that the Ni/C catalyst showed a rapid decrease in performance, but no precise information of the catalyst was given.

It is well known that bimetallic catalysts can be advantageous over the monometallic systems to achieve higher activity and stability [12,26]. And it was found that bimetallic Ni–Pt catalyst was more active and stable than monometallic Ni catalyst in many hydrogenation reactions [26,27]. As for DBFC applications, Gyenge et al. [28] indicated that NiPt/C (mole ratio = 1:1) catalyst was more active than Pt/C as anode catalyst for DBFC. And Jamard et al. [29] found that the NiPt/C (mole ratio = 1:1) anode catalyst for DBFC represented higher coulombic efficiency than Pt/C anode catalyst. However, only one component of the Ni–Pt/C catalyst was evaluated. And the preparation methods, compositions and physical characterizations of the Ni–Pt/C catalyst, on which the catalyst performance critically depended on, were rarely studied.

* Corresponding author. Tel.: +86 411 84379072; fax: +86 411 84665057.
E-mail address: zhanghm@dicp.ac.cn (H. Zhang).

0378-7753/$ – see front matter © 2008 Elsevier B.V. All rights reserved.
doi:10.1016/j.jpowsour.2008.09.010

In our present work, different amount of Pt was added to the Ni/C catalyst for the anode of DBFC. The influence of Pt on the physical characterizations of the Ni–Pt/C catalysts was tested. And the corresponding electro-catalytic activities towards borohydride oxidation were evaluated not only by basic electrochemical measurement such as cyclic voltammetry and chronopotentiometry, but also by the practical borohydride fuel cell tests. In addition, the hydrogen evolution behaviors of the Ni–Pt/C catalysts were also investigated by the fuel cell tests.

2. Experiment

2.1. Preparation of the anode catalysts

A series of Ni–Pt/C and Ni/C catalysts were prepared by hydrazine reduction of H_2PtCl_6 and Ni $(NO_3)_2$ in ethylene glycol (EG). All of the catalysts were prepared with total metal loading of 40 wt.%. The catalyst with Ni:Pt mass ratio of 37:3 was typically prepared as follows: 90 mg Vulcan XC-72R carbon black (Cabot Corp., $S_{BET} = 250\ m^2\ g^{-1}$) was added to 60 ml EG and stirred vigorously to obtain slurry. Then solutions of 0.157 ml of 0.1463 M H_2PtCl_6 in EG, 5.55 ml of 0.17 M $Ni(NO_3)_2$ in EG were mixed and subsequently added to the slurry. The mixture was ultrasonicated for 30 min and then stirred for another 30 min, followed by the addition of 1 M NaOH to increase the pH to 10.5. The resulting mixture was kept at 60 °C and then 1 ml hydrazine was added. The reaction mixture were stirred for about two hours before the carbon supported Ni–Pt catalysts were filtered off, washed copiously with ethanol and dried in a vacuum oven at 80 °C and stored in N_2 atmosphere. The catalyst thus obtained was denoted as Ni_{37}–Pt_3/C. Carbon supported Ni catalyst and carbon supported Ni–Pt catalysts with Ni:Pt mass ratios of 35:5 and 30:10 were prepared in the same way and were denoted as Ni/C, Ni_{35}–Pt_5/C and Ni_{30}–Pt_{10}/C, respectively. For comparison, carbon supported Pt catalyst (Pt/C) was also prepared in the same way.

2.2. Preparation of membrane electrode assembly (MEA)

The core part of the DBFC consisted basically of two electrodes (anode and cathode) separated by a Na^+ form Nafion 212 membrane (Du Pont). The borohydride and hydroxide crossover could be minimized by the choice of the cation-exchange membrane.

The anode catalyst (75 mg) was mixed with 4 ml ethanol and 167 mg of 5% Nafion solution and ultrasonicated to form ink-like slurry. An appropriate amount of the slurry was then applied to a 3 cm × 6 cm Toray TGPH-060 carbon paper and dried at 80 °C for 30 min in a vacuum oven to obtained metal loading of 1.0 mg cm^{-2} on the electrode surface.

In this paper, the cathodes adopted the commercial 46 wt.% Pt/C (TKK Corp.) with Pt loading of 1 mg cm^{-2}. A Teflonized (25%) SGL carbon paper with a thin microporous layer of Vulcan XC-72R carbon black, bound with 20 wt.% PTFE was used as the cathode diffusion layer and a mixture including catalysts, PTFE and ethanol was spread on the diffusion layer as the catalyst layer. Finally, a thin layer of Nafion solution (0.8 mg Nafion cm^{-2}) was spread onto the surface.

2.3. Single cell tests

For single cell tests, the effective geometrical area of all the anodes and cathodes was 5 cm^2 and the catalyst loading was 1 mg metal cm^{-2}. Details of the testing system of the single fuel cell were described in Fig. 1. An alkali $NaBH_4$ borohydride solution containing 5 wt.% $NaBH_4$ and 10 wt.% NaOH was fed to the anode

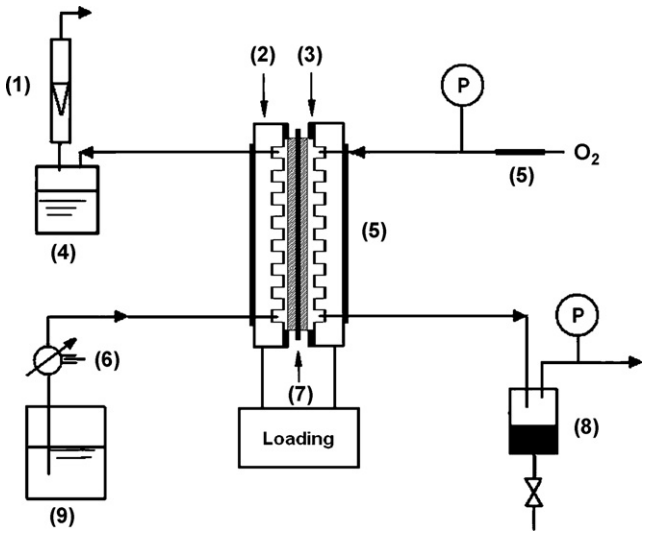

Fig. 1. Schematic test system for the DBFC. (1) Flow meter (2) bipolar plate (3) seal material (4) borohydride recovery tank (5) heater (6) qualitative fuel pump (7) MEA (8) NaOH sol. trap (9) fuel tank.

inlet at a flow rate of 1 ml min^{-1} by a qualitative fuel pump. Oxygen gas was fed to the cathode inlet at a flow rate of 0.1 l min^{-1} without humidification. And the oxygen pressure was 0.2 Mp. The open-circuit voltages (OCVs) of the DBFC were measured when the cell voltages were stable. Cell polarization measurements were conducted by applying constant current for 2 min at each point. And the amount of hydrogen produced during operation was measured using a flow meter and the volume was converted into the value at the standard temperature and pressure.

2.4. Half-cell tests

The electrochemical oxidation of borohydride on the catalysts was studied by cyclic voltammetry (CV) and chronopotentiometry. An EG & G 263 potentiostat/galvanostat was used for the electrochemical measurements in a three-electrode test cell. The working electrode was a thin porous coating disk electrode with a diameter of 3 mm. An Hg/HgO, 2 M NaOH electrode (abbreviated as MOE) was used as reference, whilst the counter electrode was a graphite rod (exposed area = 5.5 cm^2). The potential of the Hg/HgO reference electrode was 0.129 V with respect to NHE reference electrode. Thin porous coating disk electrode design was similar to that described in a previous paper [12]. About 2.5 mg catalyst was ultrasonically suspended in 1.0 ml isopropanol and 10 μl Nafion (5 wt.%) solution for about 30 min to obtain the catalyst ink, then 20 μl of the catalyst ink was spread onto the surface of a clean glass carbon electrode and dried at room temperature. The electrochemical experiments were carried out in 2 M NaOH solution containing 0.2 M $NaBH_4$, which was deaerated by ultrahigh-purity nitrogen before each experiment. All the experiments were carried out at room temperature (20 ± 0.5 °C).

2.5. Physical characterizations of the catalysts

A Philips CM-1 Power X-ray diffractometer was employed using Cu Kα source (k = 1.54056 Å) to obtain XRD spectra of the catalysts. The tube current and voltage were 100 mA and 40 kV, respectively. The angle extended from 20° to 90° and varied at a rate of 5° min^{-1}. Scherrer's formula was employed to obtain the average particle size.

Transmission electron microscopy (TEM) measurements were performed on JEOL JEM-2011 operating at 120 kV. For each sample,

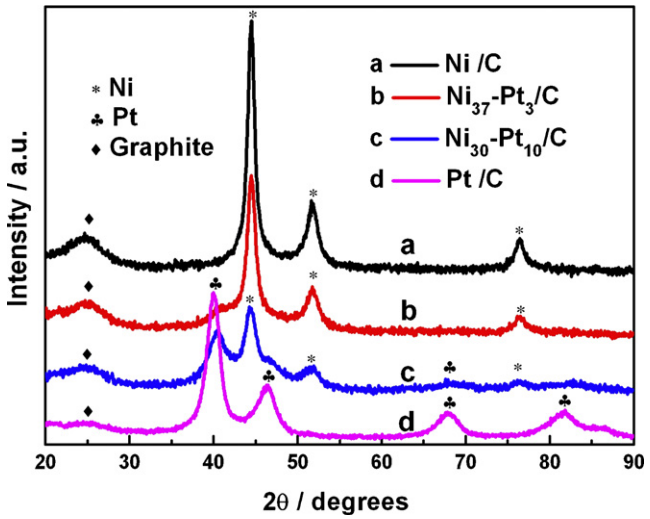

Fig. 2. XRD patterns of different catalysts.

the catalyst powder was ultrasonically suspended in ethanol and a drop of the suspension was applied to a copper grid and the ethanol was allowed to evaporate.

3. Results and discussion

3.1. Physical characterizations

X-ray diffraction patterns of the anode catalysts employed in this study were shown in Fig. 2a–d. fcc Pt and fcc Ni have distinctive diffractions and hence can be differentiated. The XRD of nickel is characterized by three peaks at $2\theta = 44.5^\circ$ (1 1 1), 51.8° (2 0 0) and 76.4° (2 2 2), while that of fcc Pt by peaks at $2\theta = 39.9^\circ$ (1 1 1), 46.2° (2 0 0), 67.9° (2 2 0), 81.5° (3 1 1) and 86.1° (2 2 2). It was clearly seen that Ni/C sample represented the typical Ni fcc crystal structure, except that the first broad peak at $2\theta = 26^\circ$ was associated with the Vulcan XC-72 support. It was also obvious that the XRD pattern of Ni_{30}–Pt_{10}/C catalyst combined the crystal features of Ni and Pt, indicating the coexistence of both of them. However the XRD pattern of Ni_{37}–Pt_3/C displayed primarily the characteristics of fcc Ni except a very small peak at $2\theta = 39.9^\circ$ with respect to Pt (1 1 1). And the corresponding peak-width of Ni in sample Ni_{37}–Pt_3/C was much bigger than that of Ni/C sample, indicating that the nanoparticles in Ni_{37}–Pt_3/C catalyst were smaller than those in Ni/C catalyst. According to Scherrer's formula, the obtained average nanoparticle sizes of Ni/C and Ni_{37}–Pt_3/C were 91.8 and 59.6 nm, respectively.

To further elucidate the morphologies of these catalysts, the TEM images had been obtained as shown in Fig. 3. Although the estimation of particle sizes in the catalysts was unclear, a reasonable agreement was seen with the values derived from the XRD results. As shown in Fig. 3A, most of the nanoparticles in Ni/C were about 100 nm. As for Ni_{37}–Pt_3/C in Fig. 3B, the nanoparticles appeared to be much smaller and more homogeneous. By the results of XRD and TEM of these two samples, it could be concluded that adding a small amount of Pt to the Ni/C catalyst led to formation of smaller nanoparticles.

The carbon supported Ni–Pt catalysts were prepared by chemical reduction of corresponding metal precursors using hydrazine in EG. The co-reduction reactions could be summarized as follows:

$$PtCl_6^{2-} + N_2H_4 + 4OH^- \rightarrow Pt + N_2 + 6Cl^- + 4H_2O$$

$$2Ni^{2+} + N_2H_4 + 4OH^- \rightarrow 2Ni + N_2 + 4H_2O$$

In their attempt to prepare PtNi nanoparticles by hydrazine reduction, Deivaraj et al. [30] proposed that the formation of PtNi nanoparticles went through two steps: the formation of Pt nanoparticle seeds at first and then the simultaneous reduction of $(PtCl_4)^{2-}$ and Ni^{2+} ions to result in bimetallic PtNi nanoparticles. Furthermore, Kumbhar and Rajadhyaksha [31] noted that the presence of Pt in bimetallic NiPt nanoparticles catalyzed the reduction of Ni^{2+} to Ni^0 due to a strong synergistic effect. Thus it could be proposed that the addition of platinum accelerated the reduction of the metal precursors and the nucleation of the metal clusters. Therefore the nanoparticles formed in Ni_{37}–Pt_3/C catalyst were smaller and more homogeneous than those in Ni/C catalyst, as it is generally agreed that the size of metal nanoparticles is determined by the reduction rate of the metal precursors [32].

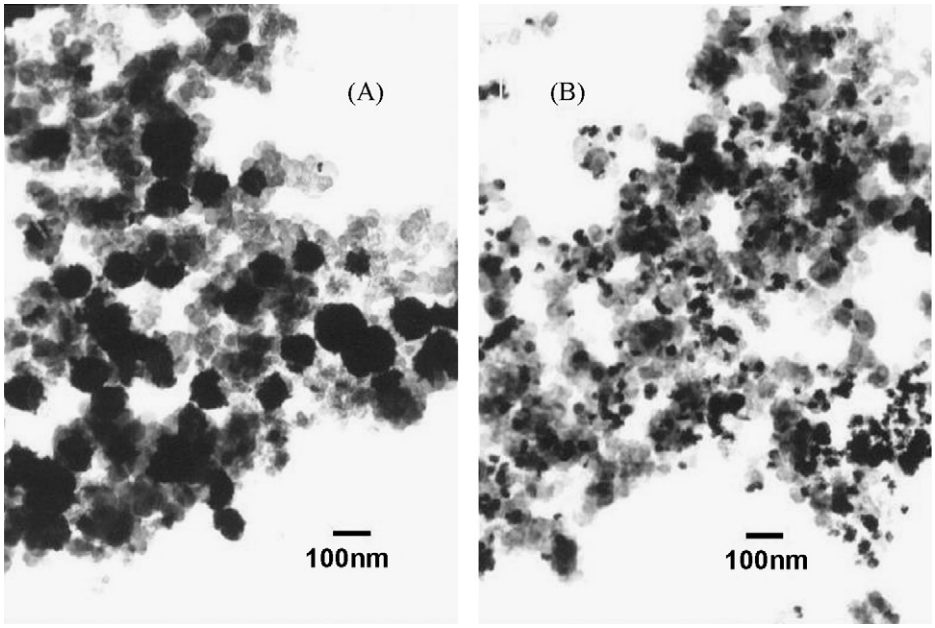

Fig. 3. TEM images of the catalysts: (A) Ni/C and (B) Ni_{37}–Pt_3/C.

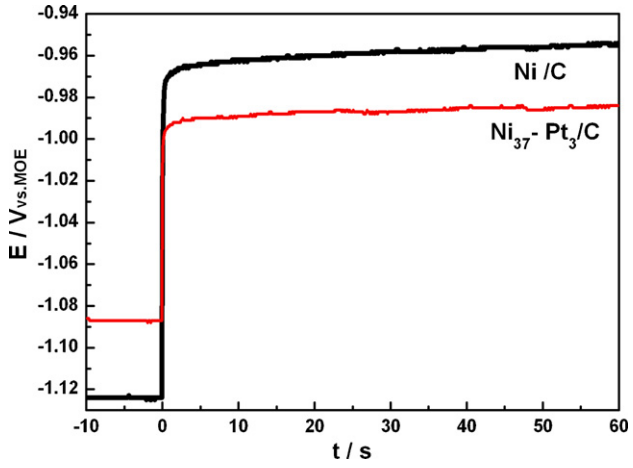

Fig. 4. Chronopotentiometry of BH_4^- oxidation on different catalysts. Current step: from 0 to 10 mA cm^{-2}; 0.2 M $NaBH_4$ in 2 M NaOH; 293 K.

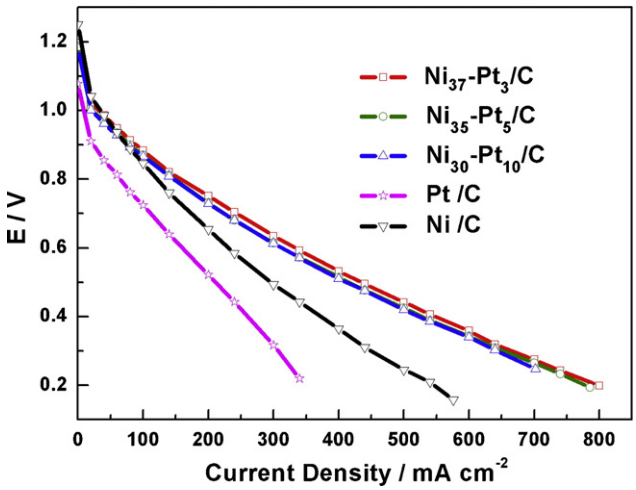

Fig. 6. Cell polarization curves of the DBFC using different anode catalysts at 60 °C. Anode catalyst loading: 1 mg metal cm^{-2}, 1 ml min^{-1} 5 wt.% $NaBH_4$ in 10 wt.% NaOH. Cathode catalyst loading: 1 mg Pt cm^{-2}, dry O_2 at 0.1 l min^{-1} (2 atm).

3.2. Half-cell tests

3.2.1. Chronopotentiometry

Chronopotentiometry is a useful catalyst screening method since it simulates the constant current operation of a fuel cell [12]. Both the open-circuit potentials (OCPs) and the potentials at 10 mA cm^{-2} for the investigated Ni/C and Ni_{37}–Pt_3/C electrodes in the half-cell tests were shown in Fig. 4. The open-circuit potentials of the electrodes were found to depend on the electrocatalysts. But the observed OCPs were all less negative than the reversible potential, while more negative than the hydrogen potential. It might be caused by the fact that the open-circuit potentials were essentially mixed potentials with contributions potentially from species such as some intermediate oxidation products of BH_4^-, especially atomic hydrogen generated by the hydrolysis of BH_4^-. And it was found that the Ni_{37}–Pt_3/C electrode exhibited less negative OCP than the Ni/C electrode, which might be due to their different catalytic activities towards the electrochemical and hydrolysis reaction of borohydride ions, boron-containing intermediates and atomic hydrogen [18]. When a current step from 0 to 10 mA cm^{-2} was applied, the operating potential of Ni_{37}– Pt_3/C electrode was more negative than that of Ni/C electrode (Fig. 4), which suggested the possibility of obtaining a higher power output with the Ni_{37}–Pt_3/C anode in the single cell test.

Table 1
Cell potentials and peak power densities of the DBFC using different anode catalysts.

Anode catalyst	OCV (V)	Potential at 300 mA cm^{-2} (V)	Peak power density (mW cm^{-2})
Ni/C	1.250	0.494	150.6
Ni_{37}–Pt_3/C	1.208	0.635	221.0
Ni_{35}–Pt_5/C	1.196	0.614	212.5
Ni_{30}–Pt_{10}/C	1.183	0.613	210.0
Pt/C	1.078	0.317	106.3

3.2.2. Cyclic voltammetry

Cyclic voltammetry under forced convection of borohydride solution was done in 2 M NaOH solution containing 0.2 M $NaBH_4$ and cycled at a scan rate of 50 mV s^{-1} and a rotating speed of 1600 rpm. Fig. 5A showed a typical CV curve obtained on the Ni_{37}–Pt_3/C electrode compared with that obtained on the Ni/C electrode between −1.15 and 0.05 V versus MOE at room temperature. The main CV feature of BH_4^- electro-oxidation on Ni/C electrode in the initial anodic scan was the peak at ca. −0.51 V, and no anodic peak was observed in the reverse scan. The phenomenon might be caused by the formation of oxidized nickel film on the electrode surface, on which BH_4^- had no electrochemical activity, as discussed by Dong et al. [1]. When the potential reached the range in which a surface oxidation reaction occurred, the surface would be oxidized and the anodic oxidation of borohydride could not continue without the active electrocatalyst. In the case of Ni_{37}–Pt_3/C electrode, the current was larger than that of Ni/C

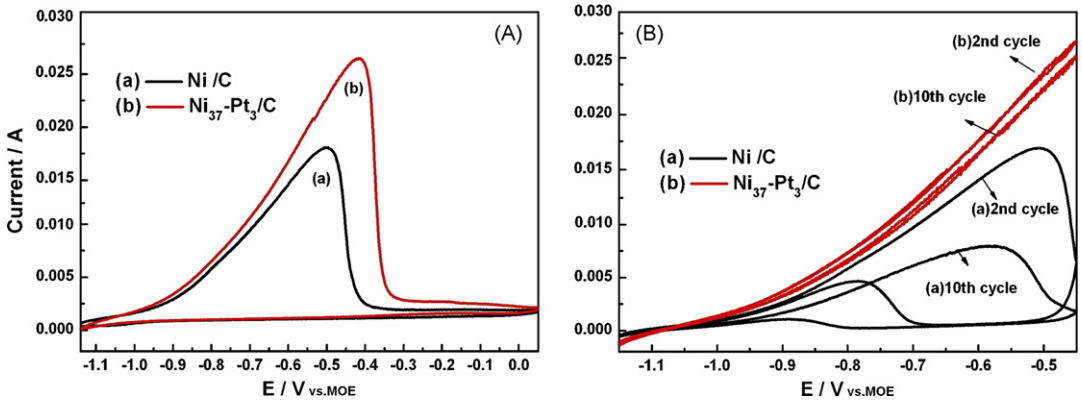

Fig. 5. Cyclic voltammograms of BH_4^- oxidation on different catalysts. Scan rate: 50 mV s^{-1}; rotating speed: 1600 rpm; $NaBH_4$ concentration: 0.2 M $NaBH_4$ in 2 M NaOH; 293 K.

electrode at the same potential, suggesting that Ni_{37}–Pt_3/C catalyst was more active than Ni/C catalyst. In order to confirm the influence of Pt addition on the stability of the catalyst, the CV curves from −1.15 to −0.45 V on the Ni/C and Ni_{37}–Pt_3/C electrodes before and after 10 cycles were presented in Fig. 5B. It can be clearly seen that the stability of the catalyst was improved by the addition of Pt.

3.3. Single cell performances

In order to evaluate the influence of Pt in the Ni–Pt/C catalysts on the cell performances, catalysts with different Pt contents: Ni/C, Ni_{37}–Pt_3/C, Ni_{35}–Pt_5/C, Ni_{30}–Pt_{10}/C and Pt/C, were used as the anode catalysts for DBFC. Fig. 6 showed the performances of the single cells with different catalysts at 60 °C. The open-circuit voltages (OCVs) of the DBFC were found to depend on the anode electrocatalysts, as shown in Table 1. The OCV of the DBFC decreased with the increasing Pt content in the catalysts. The lowest OCV, which approximated to that of PEMFC, was observed on Pt/C anode. It can be explained by the fact that with Pt most of the borohydride ions hydrolyzed as they met a catalytic particle. H_2 was released which would be electro-oxidized very fast *in situ*, and the observed OCV was a mixed potential approximated to H^+/H_2 potential. These results were in agreement with the results obtained by chronopotentiometry.

The best polarization performance of the DBFC was obtained on the Ni_{37}–Pt_3/C anode, e.g., 0.635 V at 300 mA cm^{-2} and 60 °C. Under identical condition the Ni/C anode catalyst yielded only 0.494 V, apparently confirming the results in chronopotentiometry. The particle size of the catalyst was reduced by the addition of Pt to Ni/C catalyst. This gave rise to more active sites, thereby leading to higher power density of Ni–Pt/C than that of Ni/C. However, Pt catalyst showed less negative potential than Ni catalyst towards borohydride oxidation under the employed condition, as reported by other researchers [16,18]. So the activity of the catalyst system would decrease with increasing the Pt content. If both phenomena were operating simultaneously, one would expect the power density to pass though a maximum with increasing Pt loading. The maximum power density, 221.0 mW cm^{-2}, was obtained on the Ni_{37}–Pt_3/C anode (total metal loading, 1 mg cm^{-2}) at 500 mA cm^{-2} and 60 °C (Fig. 7). This was a promising result from the view of power output, and the mass specific activity of the anode catalyst in the present work was much higher than previous reports [16,17,29]. Table 2 summarized some of the representative researches on DBFC which have been conducted since 1999.

3.4. Hydrogen evolution

Hydrogen evolution usually occurred during the operation of the DBFC [17,18,23,29], which not only reduced columbic efficiency

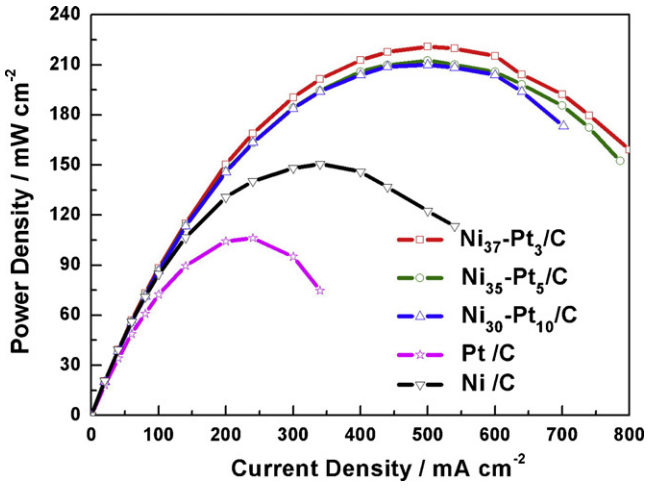

Fig. 7. Power density curves of the DBFC using different anode catalysts at 60 °C. Anode catalyst loading: 1 mg metal cm^{-2}, 1 ml min^{-1} 5 wt.% $NaBH_4$ in 10 wt.% NaOH. Cathode catalyst loading: 1 mg Pt cm^{-2}, dry O_2 at 0.1 l min^{-1} (2 atm).

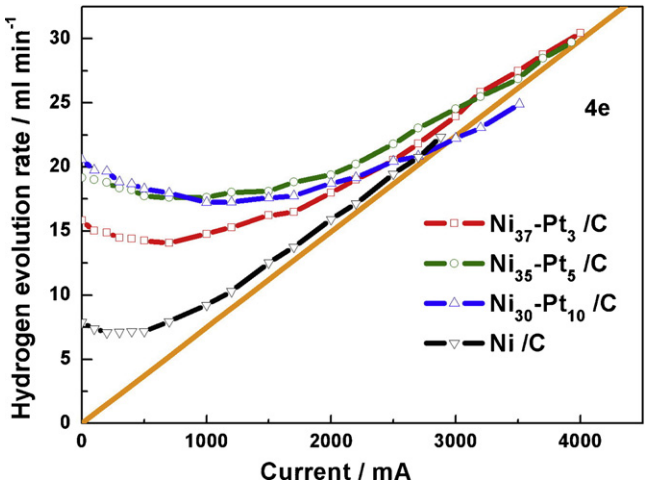

Fig. 8. Hydrogen evolution behaviors of the DBFC using different anode catalysts at 60 °C. Anode catalyst loading: 1 mg metal cm^{-2}, 1 ml min^{-1} 5 wt.% $NaBH_4$ in 10 wt.%, NaOH. Cathode catalyst loading: 1 mg Pt cm^{-2}, dry O_2 at 0.1 l min^{-1} (2 atm).

but also caused other problems such as safety problems of the fuel cell system. Hydrogen evolution behaviors based on the relation of hydrogen evolution rate and the operation current of the DBFC on the Ni-based electrodes were reported in Fig. 8. On the Ni/C electrode, it was agreed that the BH_4^- electro-oxidation was a 4e process rather than the ideal 8e reaction shown in Eq. (1) [1,18–20]:

$$BH_4^- + 4OH^- \rightarrow BO_2^- + 2H_2O + 2H_2 + 4e^- \quad (3)$$

Table 2
Various studies since 1999 on DBFC.

Ref.	Anode	Cathode	Membrane	Compositions of $NaBH_4$ solution	Cell performance
[13]	97% Au + 3%Pt	An oxygen fed cathode	Anion-exchange membrane	5% $NaBH_4$ in 25% NaOH	60 mW cm^{-2} at 70 °C
[33]	Zr–Ni alloy (200 mg cm^{-2})	Pt-black (1 mg Pt cm^{-2})	Nafion 117	10% $NaBH_4$ in 20% NaOH	0.8 V at 100 mA cm^{-2} at 60 °C
[16]	Ni powder (167 mg cm^{-2})	Pt/C (1 mg Pt cm^{-2})	Nafion NRE211	5% $NaBH_4$ in 6 M NaOH	40 mW cm^{-2} at 25 °C
[17]	14.4 mg Ni cm^{-2} + 0.6 mg Pd cm^{-2}	Pt/C (1 mg Pt cm^{-2})	Nafion 112	10% $NaBH_4$ in 20% NaOH	250 mW cm^{-2} at 60 °C
[29]	Pt–Ni/C (mole, 1:1) (5 mg catalyst cm^{-2})	Pt (4 mg Pt cm^{-2})	Nafion 117	2 M $NaBH_4$ in 1 M NaOH	0.53 V at 100 mA cm^{-2} at 60 °C
[28]	Pt–Ni/C (mole, 1:1) (0.8 mg metal cm^{-2})	Pt/C (1.3 mg Pt cm^{-2})	Anion-exchange membrane (Morgane® ADP)	2 M $NaBH_4$ in 1 M NaOH	120 mW cm^{-2} at room temperature

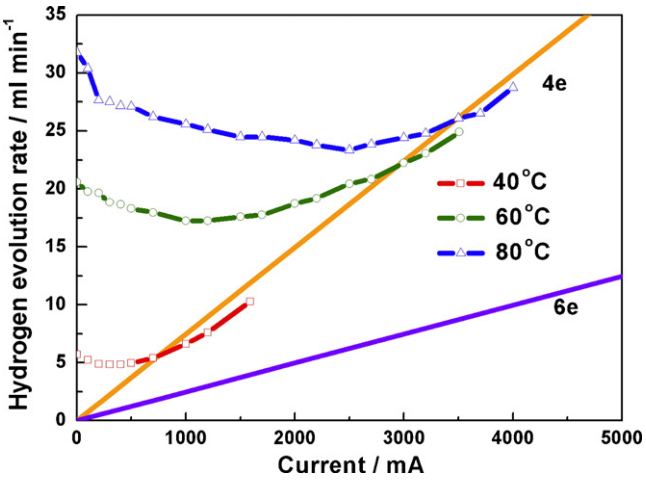

Fig. 9. Hydrogen evolution behaviors of the DBFC using Ni_{30}–Pt_{10}/C anode at different temperatures. Anode catalyst loading: 1 mg metal cm^{-2}, 1 ml min^{-1} 5 wt.% $NaBH_4$ in 10 wt.% NaOH. Cathode catalyst loading: 1 mg Pt cm^{-2}, dry O_2 at 0.1 l min^{-1} (2 atm).

As shown in Fig. 8, the hydrogen evolution rate on the Ni/C electrode was influenced by the discharge current density. The hydrogen evolution rate decreased first and then increased with the increasing anodic current and finally fell into the stoichiometric relation of 4e reaction, indicating that the highest columbic efficiency on Ni/C would not be more than 50%, if the evolved hydrogen was not further used. As for Ni_{37}–Pt_3/C electrode, the hydrogen generation rate at current <3000 mA was higher than that on the Ni/C electrode, because the smaller nanoparticles in Ni_{37}–Pt_3/C electrode not only benefited the borohydride electro-oxidation but also benefited the borohydride hydrolysis. But with the current increasing, the columbic efficiency increased and the highest columbic efficiency obtained on the Ni_{37}–Pt_3/C electrode was 50% at 60 °C. However, Jamard et al. [29] mentioned that NiPt (mole ratio = 1:1) electrode demonstrated a higher columbic efficiency, approximately 69% of the theoretical value at room temperature. It was proposed that the different columbic efficiencies might be caused by the following reasons: (1) the different Pt contents in the Ni–Pt/C catalysts; (2) the different operation temperature. In order to confirm these, the relations of hydrogen generation rates with Pt content of the catalysts and with temperature were evaluated and shown in Figs. 8 and 9.

As shown in Fig. 8, at low operation current (<3000 mA), the generation rate of hydrogen increased with the increasing Pt content of the Ni–Pt/C electrode. But at high operation current (>3000 mA), the generation rate of hydrogen decreased with the increasing Pt content of the Ni–Pt/C electrode and the highest columbic efficiency was 51% obtained on the Ni_{30}–Pt_{10}/C electrode, suggesting that the addition of Pt contributed to increasing coulombic efficiency of the DBFC at high overpotential. This might be caused by the further oxidation of atom hydrogen on Pt nanoparticles at high overpotential, as it is known that Pt is the best catalyst for hydrogen electro-oxidation. Furthermore at high overpotential, the anodic reaction was very fast and led to low BH_4^- concentration on the anode surface, which benefited the 8e reaction of borohydride [17,18].

Fig. 9 showed the influence of operation temperature on the hydrogen evolution rate on the Ni_{30}–Pt_{10}/C anode. It can be seen that increasing the fuel cell temperature led to the increasing of hydrogen evolution rate, but the highest columbic efficiency did not change with the operation temperature, indicating that the BH_4^- electro-oxidation mechanism on the Ni_{30}–Pt_{10}/C anode did not change with temperature.

4. Conclusions

In summary, the following conclusions can be made:

1. Carbon supported Ni and Ni–Pt catalysts were prepared by hydrazine reduction of Pt and Ni precursors in EG. It was found that addition of ultra low amount of platinum (mass ratio, Ni:Pt = 37:3) to Ni/C catalyst led to the formation of smaller and more highly dispersed nanoparticles.
2. The Ni–Pt/C catalysts were found to be more active than the Ni/C catalyst towards borohydride electro-oxidation. The cell with Ni_{37}–Pt_3/C (total metal loading, 1 mg cm^{-2}) anode showed promising performance with a maximum power density of 221.0 mW cm^{-2} at 60 °C.
3. The stability of bimetallic Ni–Pt/C catalysts was found to be superior to that of monometallic Ni/C catalyst for electro-oxidation of borohydride.
4. The addition of Pt could increase the coulombic efficiency at high overpotential during the operation of the DBFC. But the efficiency was still not satisfied, and extensive investigations should be done.

References

[1] H. Dong, R.X. Feng, X.P. Ai, Y.L. Cao, H.X. Yang, C.S. Cha, J. Phys. Chem. B 109 (2005) 10896–10901.
[2] E. Gyenge, Electrochim. Acta 49 (2004) 965–978.
[3] J.I. Martins, M.C. Nunes, R. Koch, L. Martins, M. Bazzaoui, Electrochim. Acta 52 (2007) 6443–6449.
[4] J.H. Kim, H.S. Kim, Y.M. Kang, M.S. Song, S. Rajendran, S.C. Han, D.H. Jung, J.Y. Lee, J. Electrochem. Soc. 151 (2004) A1039–A1043.
[5] M.H. Atwan, D.O. Northwood, E.L. Gyenge, Int. J. Hydrogen Energy 30 (2005) 1323–1331.
[6] H. Çelikkana, M. Şahin, M.L. Aksu, T.N. Veziroğlu, Int. J. Hydrogen Energy 32 (2007) 588–593.
[7] M. Chatenet, F. Micoud, I. Roche, E. Chainet, Electrochim. Acta 51 (2006) 5459–5467.
[8] C. Ponce-de-León, D.V. Bavykin, F.C. Walsh, Electrochem. Commun. 8 (2006) 1655–1660.
[9] M.V. Mirkin, H. Yang, A.J. Bard, J. Electrochem. Soc. 139 (1992) 2212–2217.
[10] F.A. Coowar, G. Vitins, G.O. Mepsted, S.C. Waring, J.A. Horsfall, J. Power Sources 175 (2008) 317–324.
[11] H. Cheng, K. Scott, Electrochim. Acta 51 (2006) 3429–3433.
[12] M.H. Atwan, C.L.B. Macdonald, D.O. Northwood, E.L. Gyenge, J. Power Sources 158 (2006) 36–44.
[13] S.C. Amendola, P. Onnerud, M.T. Kelly, P.J. Petillo, S.L. Sharp-Goldman, M. Binder, J. Power Sources 84 (1999) 130–133.
[14] E. Sanli, H. Çelikkan, B.Z. Uysal, M.L. Aksu, Int. J. Hydrogen Energy 31 (2006) 1920–1924.
[15] M.H. Atwan, D.O. Northwood, E.L. Gyenge, Int. J. Hydrogen Energy 32 (2007) 3116–3125.
[16] B.H. Liu, Z.P. Li, K. Arai, S. Suda, Electrochim. Acta 50 (2005) 3719–3725.
[17] Z.P. Li, B.H. Liu, J.K. Zhu, S. Suda, J. Power Sources 163 (2006) 555–559.
[18] B.H. Liu, Z.P. Li, S. Suda, Electrochim. Acta 49 (2004) 3097–3105.
[19] K. Wang, J. Lu, L. Zhuang, J. Phys. Chem. C 111 (2007) 7456–7462.
[20] B.H. Liu, Z.P. Li, S. Suda, J. Electrochem. Soc. 150 (2003) A398–A402.
[21] L.B. Wang, C.A. Ma, X.B. Mao, J.F. Sheng, F.Z. Bai, F. Tang, Electrochem. Commun. 7 (2005) 1477–1481.
[22] B.H. Liu, S. Suda, J. Alloys Compd. 454 (2008) 280–285.
[23] S.M. Lee, J.H. Kim, H.H. Lee, P.S. Lee, J.Y. Lee, J. Electrochem. Soc. 149 (2002) A603–A606.
[24] M.E. Indig, R.N. Snyder, J. Electrochem. Soc. 109 (1962) 1104–1106.
[25] H. Cheng, K. Scott, K. Lovell, Fuel Cells 6 (2006) 367–375.
[26] R.V. Malyala, C.V. Rode, M. Arai, S.G. Hegde, R.V. Chaudhari, Appl. Catal. A 193 (2000) 71–86.
[27] B. Li, S. Kado, Y. Mukainakano, T. Miyazawa, T. Miyao, S. Naito, K. Okumura, K. Kunimori, K. Tomishige, J. Catal. 245 (2007) 144–155.
[28] E. Gyenge, M. Atwan, D. Northwood, J. Electrochem. Soc. 153 (2006) A150–A158.
[29] R. Jamard, A. Latour, J. Salomon, P. Capron, A. Martinent-Beaumont, J. Power Sources 176 (2008) 287–292.
[30] T.C. Deivaraj, W.X. Chen, J.Y. Lee, J. Mater. Chem. 13 (2003) 2555–2560.
[31] P.S. Kumbhar, R.A. Rajadhyaksha, in: M. Guisnet, J. Barbier, J. Barroult, C. Bouchoule, D. Duperez, G. Perot, C. Montassier (Eds.), Heterogeneous Catalysis in Fine Chemicals III, Stud. Surf. Sci. Catal., vol. 251, Elsevier, Amsterdam, 1993.
[32] Z. Liu, J.Y. Lee, W. Chen, M. Han, L.M. Gan, Langmuir 20 (2004) 181–187.
[33] Z.P. Li, B.H. Liu, K. Arai, K. Asaba, S. Suda, J. Power Sources 126 (2004) 28–33.